The steroid receptor coactivator SRC-3 (p/CIP/RAC3/AIB1/ACTR/TRAM-1) is required for normal growth, puberty, female reproductive function, and mammary gland development

Jianming Xu*†, Lan Liao*, Guang Ning*, Hiromi Yoshida-Komiya*, Chuxia Deng‡, and Bert W. O'Malley*

*Department of Molecular and Cellular Biology, Baylor College of Medicine, Houston, TX 77030; and ‡Genetics of Development and Disease Branch, National Institute of Diabetes and Digestive and Kidney Diseases, National Institutes of Health, Bethesda, MD 20892

Contributed by Bert W. O'Malley, April 12, 2000

Steroid receptor coactivator-3 (SRC-3) is a coactivator of nuclear receptors in the SRC family as assayed *in vitro*. Here, we show that mouse SRC-3 is expressed in a tissue-specific fashion and distributed mainly in the oocytes, mammary glands, hippocampus, olfactory bulb, smooth muscle, hepatocytes, and vaginal epithelium. Genetic disruption of *SRC-3* in mice results in a pleiotropic phenotype showing dwarfism, delayed puberty, reduced female reproductive function, and blunted mammary gland development. Hormonal analysis indicates that SRC-3 plays a role in both the growth hormone regulatory pathway and the production of estrogen, which may explain the observed phenotypes. These results suggest that the physiological role of SRC-3 is different from that of SRC-1 and prove the diversity among coactivator family members.

Nuclear receptors require coactivators to mediate transcriptional activation of their target genes (for review see ref. 1). The steroid receptor coactivator (SRC) family consists of three newly identified coactivators designated SRC-1 (2), GRIP1 (TIF2/SRC-2) (1, 3, 4), and p/CIP (RAC3/ACTR/AIB1/TRAM1/SRC-3) (5–10). Results from *in vitro* analyses suggest that SRCs mediate transcriptional activation through multiple mechanisms including (*i*) direct interaction with ligand-bound nuclear receptors (1); (*ii*) direct contact with certain general transcription factors such as TFIIB and TBP (11); (*iii*) interaction with common transcriptional coactivators such as CBP, p300, and p/CAF (1); (*iv*) interaction with other coactivators such as coactivator-associated arginine methyltransferase 1 (CARM-1), cancer-amplified transcriptional coactivator ASC-2, PPARγ coactivator-1 (PGC-1), and steroid receptor RNA coactivator (SRA) (12–15); (*v*) participation in chromatin remodeling through their intrinsic histone acetyltransferase activity (7, 16); and (*vi*) enzymatic modification of other constituents of the coactivator complex (17).

The *SRC-1*, *SRC-2*, and *SRC-3* genes are located in chromosomal regions 2p23, 8q21.1, and 20q12 in humans (8, 18, 19) and 12A2-A3, 1A3-A5, and 2H2-H4 in mice (20). We have shown previously that disruption of *SRC-1* in mice causes partial resistance to multiple hormones, including estrogen, progesterone, androgen, and thyroid hormone. This resistance results in a decreased response of certain target organs to hormone stimulation (21, 22). A fusion between the *SRC-2* and *moz* genes at 8q13 and 8p1 has been identified in human acute myeloid leukemia (23). Additionally, *SRC-3* (*AIB1*) is highly amplified in 10% of primary breast cancers, and its mRNA is overexpressed in 64% of primary breast tumors (8). Furthermore, *SRC-3* amplification and overexpression correlate with the sizes of estrogen receptor (ER)- and progesterone receptor (PR)-positive breast tumors (24). Because SRC-3 can strongly enhance ERα and PR activities (5, 8), and because ovarian hormones are critical for mammary gland development and tumorigenesis (25, 26), these observations suggest that SRC-3 may play an important role in mammary gland growth, development, and tumorigenesis.

Although cellular transfection assays have suggested a functional redundancy among SRCs (1), biological specificity lies largely in spatial and temporal control of gene expression. Previous data from Northern blot analysis (4, 5, 7, 9, 10, 21, 27, 28) and *in situ* hybridization (SRC-1 only) (29) suggest that, although they are widely expressed, relative expression levels of SRCs are dependent on tissue types. To understand the functional relationship among SRCs, it is necessary to obtain a more detailed expression profile based on cell types for the SRC family members.

In this report, we show that the *SRC-3* gene expression is restricted in a tissue and cell type-specific manner. Disruption of the *SRC-3* gene in mice results in a diverse phenotype of dwarfism, delayed puberty, abnormal reproductive function, and mammary gland growth retardation. The unique SRC-3 expression pattern and distinct phenotypes identified in the SRC-3-null mice prove that members of the SRC gene family play differential roles in development and that their deletions result in distinct pathologies.

BIOCHEMISTRY

Experimental Methods

Construction of Targeting Vector. The pBluescript II SK plasmid (Stratagene) was used as a backbone vector. First, an *Xba*I/*Not*I fragment for the *lacZ* coding sequence and a *Not*I/*Hin*dIII fragment for TGK-*Neo* gene were ligated tail-to-tail into *Xba*I/*Hin*dIII cloning sites. Second, a 3-kb SRC-3 genomic DNA spanning from intron 13 to intron 15 was connected to the *neo* cassette through *Hin*dIII/*Kpn*I sites and used as the 3′ targeting arm. Third, the 5′ targeting arm, a 4.2-kb genomic DNA fragment (*Xba*I/*Bam*HI) containing part of intron 1 and part of exon 2, was fused to the 5′ end of the *lacZ* sequence through adaptive *Xba*I/*Bgl*II sites, which were located in a preinserted linker bearing *Bam*HI, *Sal*I, *Xba*I, *Eco*R V, and *Bgl*II sites. The connection caused a fusion of the 10th amino acid codon of SRC-3 in frame to the *lacZ* coding sequence. Finally, the negative selection marker gene, HSV-*TK*, was subcloned upstream of the 5′ arm between the *Bam*HI and *Sal*I sites (Fig. 1*A*).

Abbreviations: SRC, steroid receptor coactivator; ER, estrogen receptor; PR, progesterone receptor; ES, embryonic stem; X-Gal, 5-bromo-4-chloro-3-indolyl β-D-galactoside; E2, 17β-estradiol; P, progesterone; P*n*, postnatal day *n*; GH, growth hormone; IGF, insulin-like growth factor.

†To whom reprint requests should be addressed at: Department of Molecular and Cellular Biology, Baylor College of Medicine, One Baylor Plaza, Houston, TX 77030. E-mail: jxu@bcm.tmc.edu.

The publication costs of this article were defrayed in part by page charge payment. This article must therefore be hereby marked "*advertisement*" in accordance with 18 U.S.C. §1734 solely to indicate this fact.

Article published online before print: *Proc. Natl. Acad. Sci. USA*, 10.1073/pnas.120166297. Article and publication date are at www.pnas.org/cgi/doi/10.1073/pnas.120166297

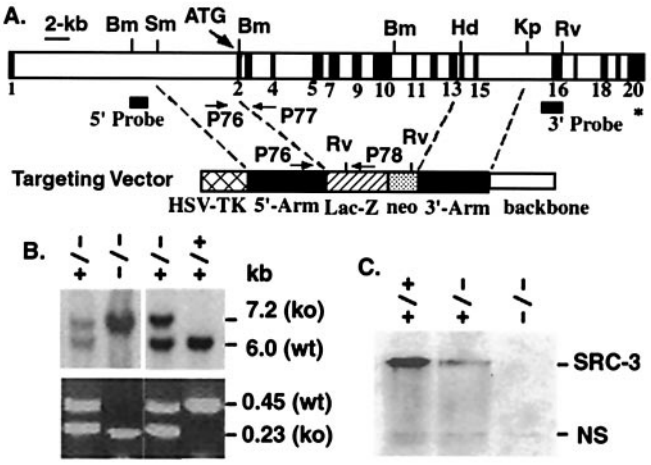

Fig. 1. Generation of SRC-3$^{-/-}$ mice. (*A*) Gene targeting strategies. Mouse SRC-3 gene is diagrammed to show its exons (black boxes), restriction enzyme sites, and codons for translational start (ATG) and stop (*). Components of the targeting vector and the corresponding locations of its 5′ and 3′ homologous targeting arms in the gene are diagrammed. Bm, *Bam*HI; Sm, *Sma*I; Hd, *Hin*dIII; Kp, *Kpn*I; Rv, *Eco*Rv. (*B*) Identification of SRC-3 mutant mice. Tail DNA was digested with *Bam*HI and *Eco*RV. Southern blotting was performed with the 5′ probe (*Upper*). The 6-kb band for wild-type allele (wt) and the 7.2-kb band for the targeted allele (ko) are indicated. In PCR analysis (*Lower*), primer pairs P76/P77 and P76/P78 (see *A* for locations) were used to detect the wild-type allele (0.45 kb) and the targeted allele (0.23 kb), respectively. (*C*) Absence of SRC-3 protein in SRC-3$^{-/-}$ mice. Western blot analysis was carried out by using tissue lysates prepared from mammary gland biopsy on lactation day 15 as described previously (21). The blot was probed with affinity-purified polyclonal Abs against human SRC-3 (37). A nonspecific (NS) band appears in all lanes and serves as a control for total amounts of protein loaded.

The targeting vector was linearized by *Bam*HI digestion and purified by phenol/chloroform extraction.

Generation of SRC-3 Mutant Mice. TC-1 embryonic stem (ES) cells were transfected with targeting vector as described previously (21, 30). Clones surviving G418 and 1-(2-deoxy-2-fluoro-β-D-arabinofuranosyl)-5-iodouracil (FIAU) selection were isolated. Targeting fidelity was determined by Southern blot analyses using probes located outside of both 3′- and 5′-targeting arms. SRC-3 mutant mice were generated from correctly targeted ES cells as described previously (21).

5-Bromo-4-chloro-3-indolyl-β-D-galactoside (X-Gal) Staining. Tissues were embedded in Tissue-Tek OCT compound (Sakura Finetechnical, Tokyo, Japan) by using dry ice. Frozen tissue sections were prepared and fixed for 5 min in PBS containing 2% paraformaldehyde, 125 mM Pipes (pH 7.3), 1 mM EGTA, and 1 mM $MgCl_2$. After washing with PBS, the sections were incubated at 30°C for 12 h in staining solution containing 1 mg/ml X-Gal, 40 mM $K_4Fe(CN)_6$, 40 mM $K_3Fe(CN)_6$, 0.6 mM sodium phosphate (pH 7.2), 0.1 M NaCl, 1 mM $MgCl_2$, and 0.2% Triton X-100. X-Gal-stained sections were further fixed in formalin for 15 min before counterstaining in nuclear fast red for 2 min. For X-Gal staining of mammary glands, tissues were fixed for 45 min in 2% paraformaldehyde, 0.25% glutaraldehyde, and 0.01% Nonidet P-40 in PBS, and stained for 12 h at 30°C in PBS containing 1 mg/ml X-Gal, 2 mM $MgCl_2$, 0.01% sodium deoxycholate, and 0.02% Nonidet P-40. The samples were then cleared in acetone, rehydrated, and stained in carmine alum overnight.

Examination of Growth and Vaginal Opening. All pups in a litter from heterozygous parents were identified individually with color markers before weaning, or ear tags after weaning. Their body weights were recorded every other day from postnatal day 3 (P3) to P28, and then once a week until P84. The data for body weight were grouped according to gender, age, and SRC-3 genotypes. Female littermates were checked for vaginal opening every day beginning at P18.

Hormone Assays. Serum samples were prepared from clotted blood specimens and stored at −80°C before assay. Serum levels of 17β-estradiol (E2) (Diagnostic Systems Laboratories, Webster, TX), growth hormone (GH; Amersham), and total insulin-like growth factor (IGF)-1 (Diagnostic Systems Laboratories) were measured by using RIA kits available commercially.

Measurement of E2- and Progesterone (P)-Stimulated Responses. To examine E2-stimulated mammary gland growth in virgin females, ovariectomy was performed on P17. Then, E2 beeswax pellets (20 μg each) or placebos were inserted under the skin on the back of the neck at day P31. After 20 days, whole mount staining of the 4th pair of mammary glands was performed (21) to examine the estrogen-dependent growth. Uterine wet weight was checked as a bioassay to ensure a successful estrogen treatment, because SRC-3 is not expressed in the endometrium. To measure the mammary gland response to a combined treatment of E2 and P, adult females were ovariectomized and treated with placebo or 21-day releasing hormone pellets containing 0.1 mg of E2 and 10 mg of P (Innovative Research of America) for 3 wk. At the end of treatment, serum concentration of E2 and uterine wet weight were measured to monitor the actual hormone release. Mammary gland morphology was examined through whole mount staining.

Examination of Reproductive Function. Superovulation and *in vivo* fertilization were examined as described previously (31). Fertilized oocytes were sorted out based on the formation of the second polar body as described (32). Examination of estrous cycle was performed on age-matched adult wild-type and SRC-3-null females. Vaginal smears were prepared for each mouse every morning and examined under the microscope. Phases of diestrus, proestrus, estrus, and metestrus during a cycle were determined according to the characteristic cell morphologies on the preparation of vaginal smears (33).

Results

Generation of SRC-3-Null Mice. Based on the organization of the mouse SRC-3 gene (20), a targeting vector was constructed to disrupt the SRC-3 gene and fuse a promoter-free *lacZ* (β-galactosidase) sequence in frame to the N-terminal coding region simultaneously (Fig. 1*A*). As confirmed by Southern blot analysis, the targeted homologous recombination in ES cells resulted in a deletion spanning from exon 2 to exon 13 (Fig. 1 *A* and *B*). The deleted region encodes amino acid residues 11–891 including the bHLH/PAS, serine/threonine-rich, and nuclear receptor interaction domains. Therefore, no functional SRC-3 protein could be produced from the targeted allele. In addition, the fusion of the *lacZ* coding sequence to the 10th amino acid of SRC-3 allows the expression of *lacZ* to be controlled by the endogenous SRC-3 promoter.

A total of 12 correctly targeted clones were identified by Southern blot analysis. Chimeric mice capable of germ-line transmission were obtained from four independent clones and were crossed to wild-type females to produce heterozygous mice. The SRC-3$^{+/-}$ mutant mice appeared normal. Heterozygotes were bred to generate SRC-3-null mice. The expected diagnostic pattern in Southern blot analysis and the absence of SRC-3 mRNA and protein clearly confirmed an authentic null mutation of the SRC-3 gene and a correct integration of the *lacZ* coding sequence in the homozygous mice (Fig. 1 *B* and *C*).

A total of 860 offspring were bred from heterozygous parents,

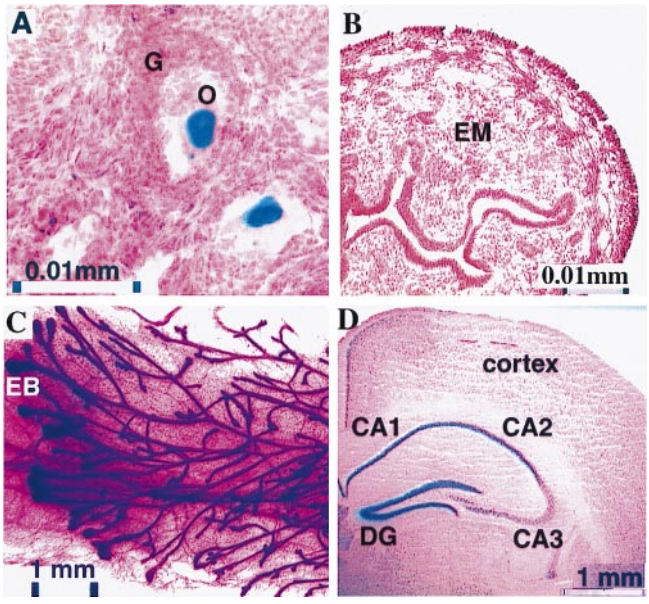

Fig. 2. Tissue-specific expression of SRC-3. Sections of frozen tissues from 4-wk-old SRC-$3^{+/-}$ mice were prepared for X-Gal staining (blue). (*A*) Ovarian section. O, oocytes; G, granulosa cells. (*B*) Cross section of the uterus. EM, uterine endometrium. (*C*) Whole mount of the mammary gland from a 6-wk-old SRC-$3^{+/-}$ female. EB, end bud. (*D*) Coronal section of the hippocampus. DG, dentate gyrus. We note that occasionally ectopic expression of β-gal can be visualized in knock-in mice. Although Northern RNA analyses of tissues are in agreement with our patterns, this remains a caveat.

including 251 SRC-$3^{+/+}$ (29%), 474 SRC-$3^{+/-}$ (55%), and 135 SRC-$3^{-/-}$ (16%) mice at weaning stage; the number of null mice (16%) was lower than that expected from Mendelian ratio (25%). In addition, the hair coat of the null mice appeared rough and dull. About 10% of the null mice exhibited wasting syndrome, including weight loss, eye and skin infection, decreased mobility, arched back, and death at various ages. These observations suggest that disruption of the SRC-3 gene in mice has a negative effect on general well-being.

SRC-3 Is Expressed in a Tissue-Specific Manner. The expression profile of SRC-3 in tissues from 4-wk-old heterozygous mice was defined with X-Gal staining. In the female reproductive system, strong SRC-3 expression was selectively detected in both oocytes (Fig. 2*A*) and smooth muscle cells of the oviduct. Low-level expression also was observed in the epithelial layer of the vagina. Surprisingly, no expression was found in the uterine endometrium (Fig. 2*B*), a tissue extremely sensitive to ovarian steroids. By contrast, in mammary gland, another target organ for ovarian steroids, high-level expression of SRC-3 was observed (Fig. 2*C*). Specifically, SRC-3 was mainly expressed in the end bud, epithelial, and myoepithelial cells of the mammary ducts. A moderate level of SRC-3 expression was detected in smooth muscle cells of both the blood vessels and intestines, and a low level of SRC-3 expression was identified in hepatocytes. In serial brain sections, high levels of SRC-3 expression were found in neurons located in the hippocampus (Fig. 2*D*), as well as the mitral cell and granule layers of the olfactory bulb. A moderate level of expression was observed in the internal granular layer of cerebellum. No detectable expression of SRC-3 was observed in the spinal cord, cardiac muscle, skeletal muscle, thymus, or pancreas.

Disruption of the SRC-3 Gene in Mice Results in Postnatal Growth Retardation. To quantify the contribution of SRC-3 to the regulation of general growth, body weight was measured. Both female and male SRC-$3^{+/-}$ mice showed the same growth rate as their wild-type littermates. However, the SRC-$3^{-/-}$ mice

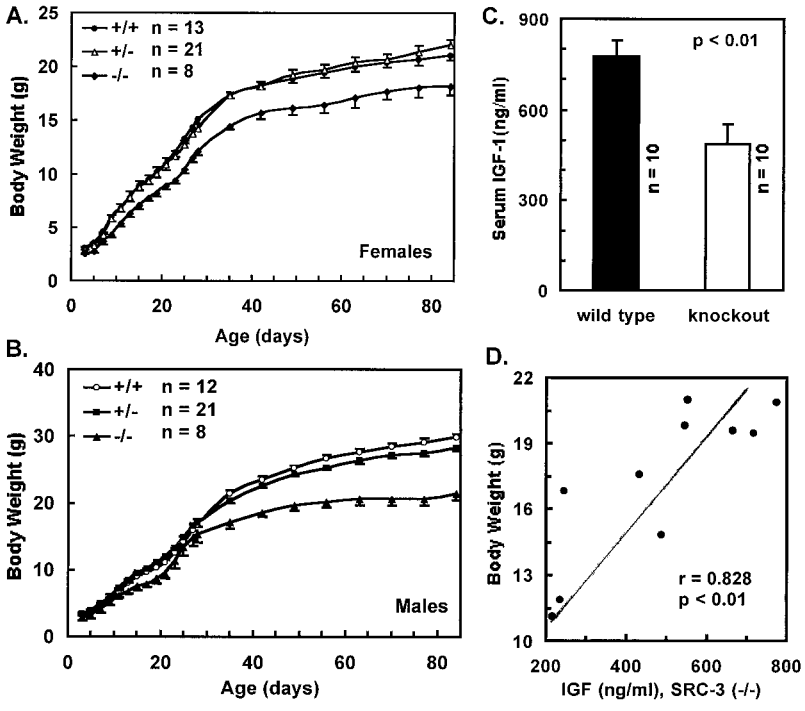

Fig. 3. SRC-$3^{-/-}$ mice exhibit growth retardation and low levels of IGF-1. (*A* and *B*) Growth curves for females and males with different SRC-3 genotypes. Body weight is presented as average ± SE. (*C*) Serum IGF-1 measurement. All mice were males with an average age of 39.3 ± 6.4 days. (*D*) Correlation between IGF-1 concentrations and body weight for SRC-$3^{-/-}$ mice. Statistical *t* test indicates a very significant ($P < 0.01$) positive correlation ($r = 0.828$).

exhibited reduced growth. The average body weight of female null mice was only 80–85% of wild-type mice (Fig. 3*A*). Statistical analysis further revealed an age-dependent progression of growth retardation for the SRC-3-null females. Before P9, there was no significant difference ($P > 0.05$, t test) in body weight among wild-type, heterozygous, and null mice. Between P9 and P21, growth rate for the null females was significantly decreased ($P < 0.05$). After P21, the SRC-3-null females showed more severe growth retardation, compared with their wild-type littermates ($P < 0.001$) (Fig. 3*A*). Similarly, male SRC-3$^{-/-}$ mice showed relatively normal growth until P28 when compared with their wild-type littermates ($P > 0.05$), followed by a severe progressive growth retardation appearing after P35 ($P < 0.001$). The average body weight of the adult SRC-3$^{-/-}$ males was 30% less than that of their control littermates (Fig. 3*B*). Our results clearly indicate that SRC-3 is required for regulation of normal growth, especially during the growth surge that accompanies pubertal development.

To investigate the physiological basis of growth retardation observed in the SRC-3$^{-/-}$ mice, we measured serum levels of GH and IGF-1, a major target of GH, in both age-matched, young wild-type, and SRC-3$^{-/-}$ mice. Although no statistical differences in GH levels could be detected between SRC-3$^{-/-}$ and SRC-3$^{+/+}$ mice, a dramatic 40% decrease in IGF-1 was detected in serum samples from SRC-3$^{-/-}$ mice (Fig. 3*C*). Further statistical calculation revealed a positive and tight correlation between the levels of IGF-1 and the body weight of individual SRC-3$^{-/-}$ mice (Fig. 3*D*). These results suggest that the IGF-1 deficiency observed may be responsible in part for the growth retardation of SRC-3$^{-/-}$ mice.

SRC-3-Null Mice Exhibit Pubertal Delay. Because growth retardation may be accompanied by pubertal delay, we compared the vaginal opening time among littermates with various SRC-3 genotypes. The mouse vaginal opening is widely used as a marker for female sexual maturation because it is regulated by estrogen and coupled to ovarian maturation, ovulation, and initiation of estrous cycle. As shown in Fig. 4*A*, the average ages of vaginal opening time were at P26.1, P26.5, and P34.4 for SRC-3$^{+/+}$, SRC-3$^{+/-}$, and SRC-3$^{-/-}$ mice, respectively, indicating a remarkable postponement of pubertal development in SRC-3$^{-/-}$ mice. At P29, wild-type females showed a well-developed vaginal epithelial layer, a large amount of secreted material in the vaginal lumen, and a wide vaginal opening. In contrast, their null littermates at the same age had a poorly developed thin vaginal epithelial layer, little secretion, and a tightly closed vagina. In agreement with the morphological characterization of the vaginal development, the serum E2 levels in SRC-3$^{-/-}$ mice reached only ≈60% of levels measured in their control littermates at P29, which was 3 days after vaginal opening in SRC-3$^{+/+}$ mice, but before vaginal opening in SRC-3$^{-/-}$ mice. Although E2 levels in SRC-3$^{-/-}$ females showed a progressive increase at later stages, it was still significantly lower than the levels in wild-type mice (Fig. 4*B*). These observations suggest that SRC-3$^{-/-}$ mice have a compromised ability to produce estrogen, which may result in delayed sexual maturation.

To test the above hypothesis, prepubertal female pups were ovariectomized on P17 and were then treated with equivalent amounts of E2. After treatment with a low dose of E2 (50 ng per mouse per day) beginning at P26, all ovariectomized mice displayed vaginal opening within 3.5 to 4.5 days, regardless of SRC-3 genotype. Because E2 therapy can rescue the delayed vaginal development, our results indicate that the pubertal delay observed in female SRC-3$^{-/-}$ mice is, at least partially, due to a decrease in systemic estrogen levels during pubertal development.

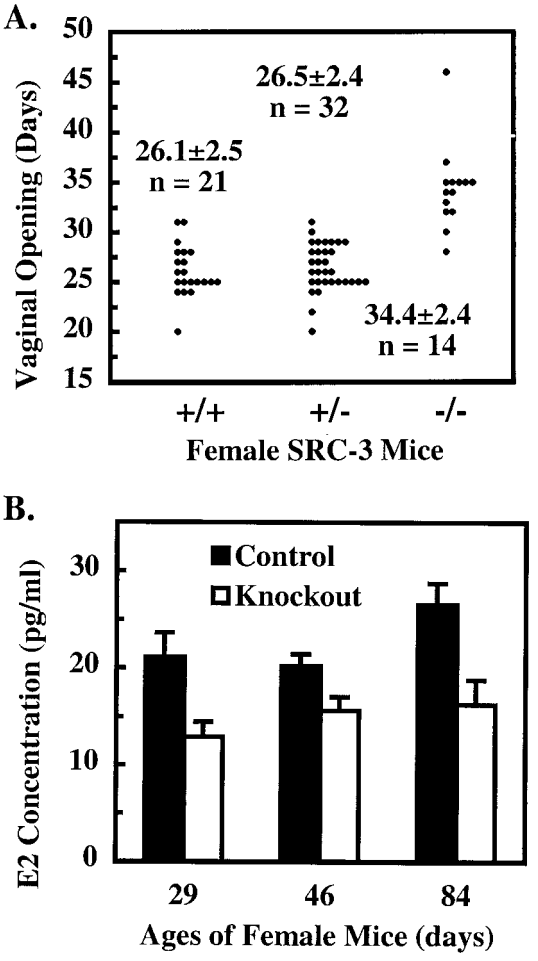

Fig. 4. SRC-3$^{-/-}$ females have delayed vaginal opening and low levels of E2. (*A*) Vaginal opening time. Individual distribution and average vaginal opening time are indicated for SRC-3$^{+/+}$, SRC-3$^{+/-}$, and SRC-3$^{-/-}$ females. There are statistical differences ($P < 0.001$) between SRC-3$^{-/-}$ and SRC-3$^{+/+}$/SRC-3$^{+/-}$ mice. (*B*) Serum E2 concentrations in control and knockout females. Control mice include wild-type and SRC-3$^{+/-}$ mice. The E2 values are presented as average ± SD ($n = 8$). E2 levels in knockout mice are statistically lower than those in control mice at all ages assayed ($P < 0.01$, t test).

SRC-3 Is Required for Normal Female Reproductive Function. First, we examined the superovulation capability and oocyte fertility. After treatment with pregnant mare's serum gonadotropin and human chorionic gonadotropin, all wild-type females were induced to superovulate and gave an average of 23.7 ± 5.5 eggs per mouse ($n = 10$). However, only 60% of SRC-3$^{-/-}$ females ovulated under the same hormonal treatment, and only 10.4 ± 3.8 eggs per mouse ($n = 10$, $P < 0.05$ vs. wild-type) were produced on average. No mature follicles were observed in the ovaries from those SRC-3$^{-/-}$ mice that did not ovulate (data not shown). When superovulated females were mated to fertile males, ovulated eggs from both wild-type and null mice showed a similar fertilization rate of ≈50%. Second, we examined the pregnancy frequency and litter sizes. After successful mating to wild-type males as determined by formation of a copulation plug, 75% of SRC-3$^{+/+}$ and SRC-3$^{+/-}$ females were pregnant. In contrast, only 36% of SRC-3$^{-/-}$ females were pregnant. Subsequently, an average of 7.3 ± 1.6 pups per litter ($n = 12$) was observed from the pregnant SRC-3$^{+/+}$ and SRC-3$^{+/-}$ females, but only 4.6 ± 0.5 pups per litter ($n = 6$, $P < 0.01$ vs. SRC-3$^{+/+}$ and SRC-3$^{+/-}$) were derived from SRC-3$^{-/-}$ mothers. Finally,

we checked estrous cycling time. Indeed, significantly prolonged estrous cycles were detected in the SRC-3$^{-/-}$ mice (14.6 ± 2.7 days, $n = 8$) as compared with their age-matched control littermates (8.1 ± 2.4 days, $n = 8$, $P < 0.001$). In conclusion, the decreased ovulation, lower pregnancy frequency, small litter size, and longer estrous cycling time clearly indicate that the SRC-3 deficient female mice have compromised reproductive function.

Mammary Gland Development Is Retarded in SRC-3-Null Mice. We first examined ductal branching and elongation during mammary gland development in virgins. In wild-type females, the mammary ducts grew rapidly upon ovarian hormone stimulation during puberty. By the age of two months, the ductal branches almost fully penetrated the mammary fat pat. At 4 wk of age, the mammary glands of both SRC-3$^{-/-}$ and SRC-3$^{+/+}$ mice showed limited growth and had no morphological differences. However, during the subsequent rapid growth stage, ductal growth in SRC-3$^{-/-}$ mice was significantly lower. By the age of 2 mo, the ductal branches penetrated only about 2/3 of the fat pat. Ductal growth in the null mice did not penetrate the entire fat pat until the age of 11 wk (data not shown). These results suggest that SRC-3 enhances mammary gland growth in a developmental stage-dependent manner.

Because mammary gland ductal growth in virgin mice depends on the estrogen signaling pathway (34, 35), and a lower level of E2 is found in SRC-3$^{-/-}$ mice (Fig. 4*B*), it was important to distinguish between local effects on ER function within the mammary gland and systemic hormonal influences. To control the serum estrogen levels, matched littermates were ovariectomized on P17, and then treated with either E2 pellets or placebo for 20 days. All placebo-treated mice showed no mammary ductal growth regardless of SRC-3 genotype (data not shown). After 20 days of E2 treatment, uterine weight was increased 10-fold for both the null and wild-type mice, confirming an expected equal response to E2 in this tissue that does not express SRC-3 (Fig. 2*B*). However, the SRC-3$^{-/-}$ mammary gland unexpectedly showed ductal growth that was similar to both wild-type and heterozygous mammary glands under the same treatment with E2 (data not shown). These results suggest that SRC-3 is not essential for ER function in stimulating virgin mammary growth. Therefore, we conclude that the reduced growth of mammary glands in SRC-3$^{-/-}$ virgins is due to insufficient systemic estrogen.

Next, we tested the ability of matured mammary glands in adult SRC-3$^{-/-}$ mice to respond to E2 + P. Thirteen-week-old, fully matured female littermates were ovariectomized and treated with slow-releasing hormone pellets containing E2 + P or placebo for 21 days. The serum level of E2 was undetectable in ovariectomized animals. In the animals treated with hormone pellets, the serum levels of E2 at the end of treatment were approximately 1.0 ng/ml and were equivalent among all treated mice. In addition, uterine endometrium was equally stimulated in all mice by hormone pellets, increasing ≈6-fold in wet weight. These observations suggest that all mice, regardless of genotypes, received identical and continuous hormonal treatment.

The mammary glands of both placebo-treated mutant and wild-type animals showed similar thin mammary ductal branches without any alveolar structures. After E2 + P treatment, the wild-type mammary glands exhibited extensive ductal arborization and alveolar formation, a phenotype similar to that observed in early pregnancy stages. In contrast, limited ductal arborization and very little alveolar development were observed in the SRC-3-deficient mammary glands under the same experimental conditions (Fig. 5). Our results indicate that the mammary ductal branching and alveolar formation in response to estrogen and P stimulation are significantly attenuated in adult female SRC-3$^{-/-}$ mice.

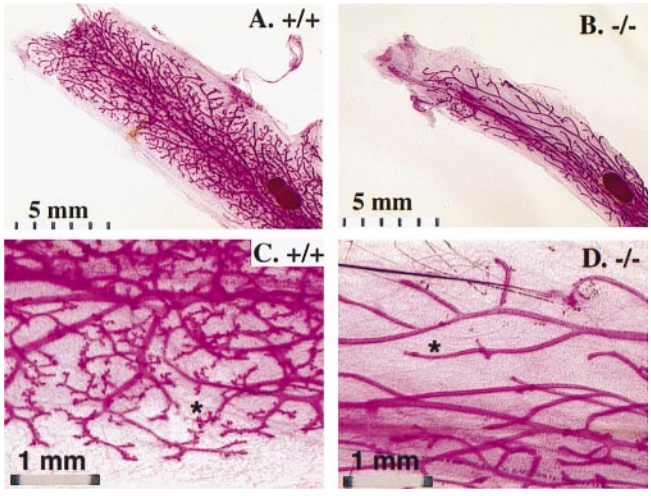

Fig. 5. E2 and P-stimulated alveolar formation is reduced in SRC-3$^{-/-}$ mammary gland. Whole mount of mammary gland was prepared from E2 + P pellet-treated adult females with indicated SRC-3 genotypes. Note the dramatic difference in the amount of aborization and the number of alveoli (*).

Discussion

The mice lacking SRC-3 exhibit retarded growth, delayed puberty, decreased reproductive function, and blunted mammary gland development. With the exception of the deficiency in mammary gland development, all other phenotypes described here were not observed in the SRC-1$^{-/-}$ mice that exhibited partial steroid and thyroid hormone resistance (21, 22). These results indicate that SRC-3 and SRC-1 have distinct roles *in vivo*, and that SRC-3 may play a more critical role in overall growth and sexual maturation.

Surprisingly, SRC-3 shows a restricted expression pattern and is present mainly in the oocytes, mammary gland ductal cells, hippocampus, olfactory bulb, and smooth muscle (Fig. 2). Previous Northern analyses using RNA from whole tissues suggested that SRC-3 was more widely expressed in different tissues, which was most likely due to the expression of SRC-3 in all vascular smooth muscle cells. When compared with SRC-1 (29), obvious differences in expression pattern exist between these two genes. For example, in the neocortex, SRC-1 is highly expressed, whereas SRC-3 has a very low level of expression; and in the cardiac muscle, SRC-1 is highly expressed whereas SRC-3 is undetectable. The differential expression patterns for SRC-1 and SRC-3 are generally consistent with the distinct phenotypes exhibited by the mice in which these individual genes have been knocked out.

Unexpectedly, disruption of the *SRC-3* gene in mice results in dwarfism. Our analyses revealed that the SRC-3$^{-/-}$ mice possess a low level of serum IGF-1. Moreover, the absolute values of IGF-1 in knockout mice positively correlate with their body weight (Fig. 3 *C* and *D*). These results indicate that SRC-3 is required for normal growth, and that the growth retardation in mice lacking SRC-3 is most likely caused by deficiency in IGF-1 production. Our study raises the question as to whether a subset of patients with growth retardation may bear *SRC-3* mutations if no alterations are detected for those genes known to cause dwarfism.

The mechanism that underlies the decrease of IGF-1 in the SRC-3$^{-/-}$ mice is unclear. Because the pulsatile fashion of GH secretion interferes with its measurement, it is still possible that the lower levels of IGF-1 observed may be due to decreased GH levels. It is also possible that the sensitivity of target cells to GH stimulation or the transcription of IGF-1 is blunted in the SRC-3$^{-/-}$ mice. In addition, it has been suggested that GH levels

may have a certain degree of correlation with E2 levels (36). Because a lower level of E2 exists in the SRC-3$^{-/-}$ mice (Fig. 4*B*), it was important to determine whether E2 therapy could rescue the IGF-1 deficiency in the SRC-3$^{-/-}$ mice. Our analysis indicates that neither the serum IGF-1 levels nor the body weight of the SRC-3$^{-/-}$ mice can be improved by the E2 treatment (data not shown). This observation suggests that the low level of E2 in the SRC-3$^{-/-}$ mice is not responsible for either the IGF-1 deficiency or growth retardation.

In contrast, the low levels of E2 are responsible for the pubertal delay in the female SRC-3$^{-/-}$ mice, because the timing for vaginal opening appears identical in both wild-type and knockout mice after treating animals with E2. These results indicate that the delayed vaginal opening in the mutant mice is due to insufficient systemic E2. These results also indicate that, whereas SRC-3 is expressed at a low level in the vaginal epithelial layer, it is not essential for response of the vaginal epithelium to E2.

The mechanism by which disruption of SRC-3 causes estrogen deficiency raises an interesting question. Because equal administration of E2 gave the same serum E2 levels and identical biological responses in terms of vaginal opening and uterine growth in both wild-type and knockout mice, the low level of E2 in knockout mice is not caused by a faster rate of E2 metabolism. It seems unlikely that the decreased E2 levels are due to an insufficient amount of gonadotropins, because no significant difference in follicle-stimulating hormone (FSH) levels could be detected between wild-type and SRC-3$^{-/-}$ mice (data not shown). Therefore, the problem may lie in the ovary, where the majority of estrogen is synthesized. In support of this hypothesis, administration of equal amounts of pregnant mare's serum gonadotropin, in contrast to administration of E2, to both wild-type and SRC-3$^{-/-}$ littermates on P23 resulted in differential responses in vaginal opening (wild-type: 48 h; knockout: 72 h after pregnant mare's serum gonadotropin injection). This result suggests that the granulosa cells in the ovary may have a reduced sensitivity to FSH. Most likely, the reduced sensitivity is due to a secondary effect of SRC-3, because its expression is undetectable in the granulosa cells (Fig. 2*A*). Because SRC-3 is highly expressed in the oocytes, this secondary effect may be elicited through an unknown interaction between the granulosa cells and oocytes.

Consistent with delayed puberty and E2 insufficiency, reproductive function in the female SRC-3$^{-/-}$ mice in terms of ovulatory capacity, litter size, and length of estrous cycle is also substantially affected. Removal of SRC-3 from the oocyte, where it is normally expressed, may directly affect oocyte development. Alternatively, reduced ovulatory capacity may be related to a hypodevelopment of the ovary because of delayed onset of puberty. The observed small litter sizes, then, would be directly related to this decreased ovulatory capability. Finally, the prolonged estrous cycle in the SRC-3$^{-/-}$ females may be a result of endocrine disturbance such as abnormal E2 levels.

It is known that the *SRC-3* (*AIB1*) gene is highly amplified and overexpressed in ER- and PR-positive human breast tumors (8, 24). Our data demonstrated that SRC-3 is highly expressed in the end bud and epithelial cells of mammary gland ducts (Fig. 2*C*). Based on these data, we proposed that SRC-3 might play an important role in mammary gland development. Indeed, we have observed that mammary gland ductal growth in SRC-3$^{-/-}$ mice is retarded. However, our results indicate that the low level of E2 is a major factor responsible for retardation of mammary ductal growth in the null mice, because estrogen therapy successfully rescues the growth deficiency of mammary ducts without changing the IGF-1 level in SRC-3$^{-/-}$ mice. These findings indicate that SRC-3 is not essential for the E2-stimulated ductal growth in the virgin mice even though it is highly expressed in mammary gland epithelial cells.

Importantly, mammary gland alveolar development in response to a combined stimulation of E2 and P is dramatically decreased in SRC-3 mutants (Fig. 5). The poorly developed morphology of the SRC-3$^{-/-}$ mammary gland is similar, although less severe, to that observed in the PR knockout mice after treatment with E2 and P (31). These results show that SRC-3 is required for P-stimulated cell proliferation and glandular differentiation during breast alveolar development.

In summary, we have shown that the SRC-3 gene has a tissue- and cell type-specific expression profile. Disruption of the *SRC-3* gene in mice results in a pleiotropic pattern of dwarfism, delayed puberty, abnormal reproductive function, and mammary gland growth retardation. Further analysis has indicated that SRC-3 is involved in the regulatory pathway for GH function and the production of estrogen. The different expression patterns of SRC-1 and SRC-3 and the distinct physical and functional phenotypes of the SRC-1 and SRC-3 knockout mice clearly indicate that members of the SRC gene family play differential roles in development and disease.

We thank F. J. DeMayo and his staff for microinjection of ES cells and mouse embryo transfer, J. Wong and R.-C. Wu for the SRC-3 polyclonal Abs, and M.-J. Tsai and K. Schillinger for aid in manuscript preparation. This research is supported by Department of Defense Grants DAMD17-00-1-0148 and -0149) to J.X. and a National Institute of Child Health and Human Development grant to B.W.O.

1. McKenna, N. J., Lanz, R. B. & O'Malley, B. W. (1999) *Endocr. Rev.* **20,** 321–344.
2. Onate, S. A., Tsai, S. Y., Tsai, M. J. & O'Malley, B. W. (1995) *Science* **270,** 1354–1357.
3. Hong, H., Kohli, K., Trivedi, A., Johnson, D. L. & Stallcup, M. R. (1996) *Proc. Natl. Acad. Sci. USA* **93,** 4948–4952.
4. Voegel, J. J., Heine, M. J., Zechel, C., Chambon, P. & Gronemeyer, H. (1996) *EMBO J.* **15,** 3667–3675.
5. Torchia, J., Rose, D. W., Inostroza, J., Kamei, Y., Westin, S., Glass, C. K. & Rosenfeld, M. G. (1997) *Nature (London)* **387,** 677–684.
6. Li, H., Gomes, P. J. & Chen, J. D. (1997) *Proc. Natl. Acad. Sci. USA* **94,** 8479–8484.
7. Chen, H., Lin, R. J., Schiltz, R. L., Chakravarti, D., Nash, A., Nagy, L., Privalsky, M. L., Nakatani, Y. & Evans, R. M. (1997) *Cell* **90,** 569–580.
8. Anzick, S. L., Kononen, J., Walker, R. L., Azorsa, D. O., Tanner, M. M., Guan, X. Y., Sauter, G., Kallioniemi, O. P., Trent, J. M. & Meltzer, P. S. (1997) *Science* **277,** 965–968.
9. Takeshita, A., Cardona, G. R., Koibuchi, N., Suen, C. S. & Chin, W. W. (1997) *J. Biol. Chem.* **272,** 27629–27634.
10. Suen, C. S., Berrodin, T. J., Mastroeni, R., Cheskis, B. J., Lyttle, C. R. & Frail, D. E. (1998) *J. Biol. Chem.* **273,** 27645–27653.
11. Takeshita, A., Yen, P. M., Misiti, S., Cardona, G. R., Liu, Y. & Chin, W. W. (1996) *Endocrinology* **137,** 3594–3597.
12. Chen, D., Ma, H., Hong, H., Koh, S. S., Huang, S. M., Schurter, B. T., Aswad, D. W. & Stallcup, M. R. (1999) *Science* **284,** 2174–2177.
13. Lee, S. K., Anzick, S. L., Choi, J. E., Bubendorf, L., Guan, X. Y., Jung, Y. K., Kallioniemi, O. P., Kononen, J., Trent, J. M., Azorsa, D., *et al.* (1999) *J. Biol. Chem.* **274,** 34283–34293.
14. Puigserver, P., Adelmant, G., Wu, Z., Fan, M., Xu, J., O'Malley, B. & Spiegelman, B. M. (1999) *Science* **286,** 1368–1371.
15. Lanz, R. B., McKenna, N. J., Onate, S. A., Albrecht, U., Wong, J., Tsai, S. Y., Tsai, M. J. & O'Malley, B. W. (1999) *Cell* **97,** 17–27.
16. Spencer, T. E., Jenster, G., Burcin, M. M., Allis, C. D., Zhou, J., Mizzen, C. A., McKenna, N. J., Onate, S. A., Tsai, S. Y., Tsai, M. J., O'Malley, B. W. (1997) *Nature (London)* **389,** 194–198.
17. Chen, H., Lin, R. J., Xie, W., Wilpitz, D. & Evans, R. M. (1999) *Cell* **98,** 675–686.
18. Carapeti, M., Aguiar, R. C., Chase, A., Goldman, J. M. & Cross, N. C. (1998) *Genomics* **52,** 242–244.
19. Kalkhoven, E., Valentine, J. E., Heery, D. M. & Parker, M. G. (1998) *EMBO J* **17,** 232–243.
20. Ning, G., Jurecic, V., Baldini, A. & Xu, J. (1999) *In Vitro Cell Dev. Biol. Anim.* **35,** 481–486.
21. Xu, J., Qiu, Y., DeMayo, F. J., Tsai, S. Y., Tsai, M. J. & O'Malley, B. W. (1998) *Science* **279,** 1922–1925.
22. Weiss, R. E., Xu, J., Ning, G., Pohlenz, J., O'Malley, B. W. & Refetoff, S. (1999) *EMBO J.* **18,** 1900–1904.
23. Carapeti, M., Aguiar, R. C., Goldman, J. M. & Cross, N. C. (1998) *Blood* **91,** 3127–3133.
24. Bautista, S., Valles, H., Walker, R. L., Anzick, S., Zeillinger, R., Meltzer, P. & Theillet, C. (1998) *Clin. Cancer Res.* **4,** 2925–2929.
25. Martin, G., Davio, C., Rivera, E., Melito, G., Cricco, G., Andrade, N., Caro, R. & Bergoc, R. (1997) *Cancer Invest.* **15,** 8–17.
26. Fishman, J., Osborne, M. P. & Telang, N. T. (1995) *Ann. N.Y. Acad. Sci.* **768,** 91–100.
27. Li, H. & Chen, J. D. (1998) *J. Biol. Chem.* **273,** 5948–5954.
28. Misiti, S., Schomburg, L., Yen, P. M. & Chin, W. W. (1998) *Endocrinology* **139,** 2493–2500.
29. Misiti, S., Koibuchi, N., Bei, M., Farsetti, A. & Chin, W. W. (1999) *Endocrinology* **140,** 1957–1960.
30. Deng, C., Wynshaw-Boris, A., Zhou, F., Kuo, A. & Leder, P. (1996) *Cell* **84,** 911–921.
31. Lydon, J. P., DeMayo, F. J., Funk, C. R, Mani, S. K., Hughes, A. R., Montgomery, C. A., Jr., Shyamala, G., Conneely, O. M. & O'Malley, B. W. (1995) *Genes Dev.* **9,** 2266–2278.
32. Hogan, B., Beddington, R., Costantini, F. & Lacy, E. (1994) *Manipulating the Mouse Embryo: A Laboratory Manual* (Cold Spring Harbor Lab. Press, Plainview, NY), p. 42.
33. Snell, G. D. (1941) *Reproduction* (Blakiston, New York), pp. 55–58.
34. Topper, Y. J. & Freeman, C. S. (1980) *Physiol. Rev.* **60,** 1049–1106.
35. Lubahn, D. B., Moyer, J. S., Golding, T. S., Couse, J. F., Korach, K. S. & Smithies, O. (1993) *Proc. Natl. Acad. Sci. USA* **90,** 11162–11166.
36. Muller, E. E., Locatelli, V. & Cocchi, D. (1999) *Physiol. Rev.* **79,** 511–607.
37. Li, J., O'Malley, B. W. & Wong, J. (2000) *Mol. Cell. Biol.* **20,** 2031–2042.